



Simulated Long-Term Vegetation–Climate Feedbacks in the Tibetan Plateau

Wei Hua^{1,2,3,4} · Zouxin Lin^{1,2,3} · Donglin Guo⁴ · Guangzhou Fan^{1,2,3} · Yongli Zhang^{1,2,3} · Kaiqin Yang^{1,2,3,4} · Qin Hu^{1,2,3,4} · Lihua Zhu^{1,2,3}

Received: 23 April 2018 / Revised: 6 August 2018 / Accepted: 11 August 2018 / Published online: 28 September 2018
© Korean Meteorological Society and Springer Nature B.V. 2018

Abstract

The Tibetan Plateau (TP) is an important region of land–atmosphere interactions with high climate variability. In this study, an atmosphere–vegetation interaction model was applied to explore the possible responses of vegetation to climate warming, and to assess the impacts of land cover change on the land surface physical processes across the TP. Results showed that long-term warming over the TP could influence vegetation growth via different mechanisms. Most likely, increased temperature would enhance the physiological activity in most high cold areas on the TP, whereas high temperature would inhibit vegetation growth by increasing respiration in areas with favorable water and temperature conditions. In addition, for areas where the climate is warmer but not wetter, higher temperature could influence photosynthesis via the moisture condition of the vegetation rather than by modulating respiration. Numerical simulations demonstrated that vegetation could control the land surface–atmosphere energy balance effectively. The change of land cover from vegetated land to desert steppe decreased the net radiation absorbed by the surface, weakening the surface thermal effects, and reducing sensible and latent heat fluxes. Furthermore, sensitivity simulations also revealed that global warming would likely accelerate vegetation growth in most areas of the TP, resulting in increased surface heat flux.

Keywords Vegetation–climate feedback · Climate change · Vegetation physiological process · Surface heat flux · Tibetan plateau

1 Introduction

In areas of high latitude and high elevation, vegetation—including high-cold steppe, grasslands, shrublands, and forest, is the main component of the land ecosystem. Thus, changes in vegetation are likely to have profound impact on ecosystem

structure, radiation balance, water and energy cycles, and climate change on regional to global scales (Crucifix et al. 2005; Notaro and Liu 2008). In addition to concerns about the effects of land cover change (LCC) on land–atmosphere energy, water, carbon, and momentum exchanges, there is a growing concern regarding the response of vegetation physiological processes to climate change. This is because vegetation physiological processes are strongly affected by climate, and because the CO₂ concentration of the atmosphere could cause considerable changes to vegetation species composition among different types (Goetz et al. 2000). For instance, the global terrestrial ecosystem structure has undergone considerable change (Cramer and Coauthors 2001) in conjunction with the rapid warming observed during recent decades (Jones et al. 2012). Other regional examples include the response of vegetation distribution to climate change in North America (Lenihan et al. 2008), Europe (Theurillat and Guisan 2001), and China (Zhao and Wu 2014). Changes in vegetation–atmosphere interaction sometimes result in an unexpected change in the climate system, most likely resulting in anomalous atmospheric circulation, vegetation zone shifts, and tree line movements, which

Responsible editor: Sang-Wook Yeh

✉ Wei Hua
huawei@cuit.edu.cn

- ¹ Joint Laboratory of Climate and Environment Change, Chengdu University of Information Technology, Chengdu, Sichuan, China
- ² Plateau Atmosphere and Environment Key Laboratory of Sichuan Province, Chengdu University of Information Technology, Chengdu, Sichuan, China
- ³ School of Atmospheric Sciences, Chengdu University of Information Technology, Chengdu, Sichuan, China
- ⁴ Nansen-Zhu International Research Centre, Institute of Atmospheric Physics, Chinese Academy of Sciences, Beijing, China

are especially evident in regions of high latitude and high elevation. For example, shifts might occur in Arctic vegetated areas to a different physiognomic class, and it has been predicted that woody cover will increase by as much as 52% under climate warming (Pearson et al. 2013). In addition, the intensity of the East Asian summer monsoon could be influenced by thermal effects attributable to vegetation greenness on the southeastern Tibetan Plateau (TP) (Zhang et al. 2011).

In China, the TP is nicknamed the “third pole” of the earth because it is the highest and largest plateau in the world with average elevation >4000 m and an area of approximately 2.0×10^6 km². It therefore exerts major influence on both regional and global atmospheric climate through thermal and dynamical forcings via land–atmosphere interactions (e.g., Yeh et al. 1957; Flohn 1957; Yanai et al. 1992; Li and Yanai 1996; Zhao and Chen 2001; Duan and Wu 2008; Wang et al. 2014, 2016, 2018). Statistically significant warming of the TP has now been detected and it is predicted to continue to warm more substantially over the next 100 years (Guo and Wang 2012; Zhou et al. 2014; Hua et al. 2017). Climate warming tends to either accelerate ecosystem change or enhance uncertainties in land surface process; thus, it is expected to project the thermal and dynamical effects of the TP to downstream areas (Hua et al. 2008; Zuo et al. 2011).

Because of growing concerns about these important issues, considerable efforts have been made to investigate the land surface processes and associated mechanisms on the TP under global warming. Using normalized difference vegetation index datasets, Zhong et al. (2010) assessed the vegetation dynamics and their responses to variations in precipitation and temperature on the TP. Furthermore, numerical simulation has also been used to study land–atmosphere interactions on the TP. With an atmospheric general circulation model, the possible impact of LCC on the summer circulation over the TP has been explored (Li and Xue 2010). The results showed that vegetation degeneration decreases surface thermal effects, leading to lower atmospheric temperatures and weaker vertical ascending motion, low-layer cyclonic, upper-level anticyclonic, and summer monsoon circulations. The studies mentioned above have provided important insights into the land–atmosphere interactions and associated mechanisms on the TP

during recent decades. Nevertheless, the detailed mechanisms of land–atmosphere interactions have not been fully assessed. In particular, some land surface models have limited capability to demonstrate dynamic atmosphere–vegetation interactions.

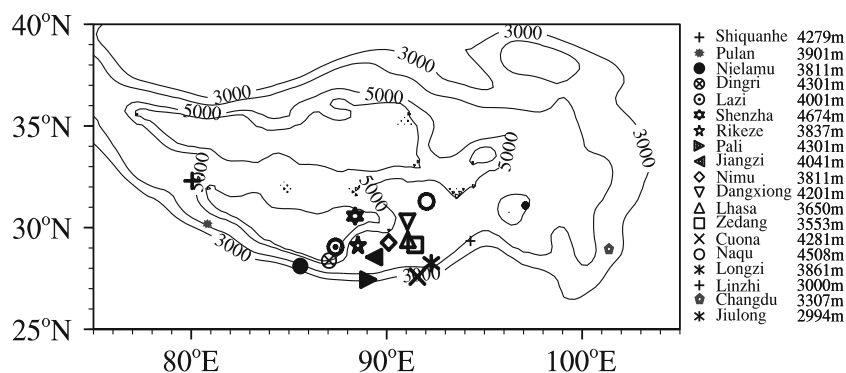
The objectives of the present study were (i) to investigate the influence of climate warming on vegetation growth and (ii) to assess the influence of plant physiological processes on surface energy exchange. A brief introduction to the TP is given in Section 2. Descriptions of the data, model and experimental design are provided in Section 3, and the results are presented in Section 4. A summary of the core findings of this study and a discussion are provided in Section 5.

2 Brief Introduction to the TP

The climate over the TP has a strong east–west gradient, which is manifest as a wet warm eastern region and a dry cold western region. The gradient of vegetation over the TP follows the gradient of climate. The western TP, such as Shiquanhe with land cover of desert steppe vegetation, receives <100 mm of precipitation annually, whereas the valleys of the southeastern TP, such as Linzhi, receive >600 mm of precipitation annually and they have evergreen coniferous forest as the typical vegetation cover. Because of these significant east–west gradients of both climate and land cover on the TP, we selected 19 meteorological stations from east to west across the TP for our simulations (Fig. 1).

Figure 2 shows the surface air temperature (Fig. 2a), total precipitation (Fig. 2b), cloudiness (Fig. 2c), and incident solar radiation (Fig. 2d) from east to west across the TP during the main growing season (May–September). There is an overall decrease in temperature from east to west and some stations have an average temperature of <8 °C (e.g., Naqu, Cuona, and Pali), which can be attributed to the high elevation (i.e., >4200 m). Precipitation across the TP is largest in eastern regions (about 790 mm at Jiulong) and smallest in western areas (only 60 mm at Shiquanhe). There is an obvious east–west decreasing gradient in cloudiness; thus, incident solar radiation is low in the east and high in the west.

Fig. 1 Locations of the selected 19 meteorological stations (dashed line denotes the topography of the TP)



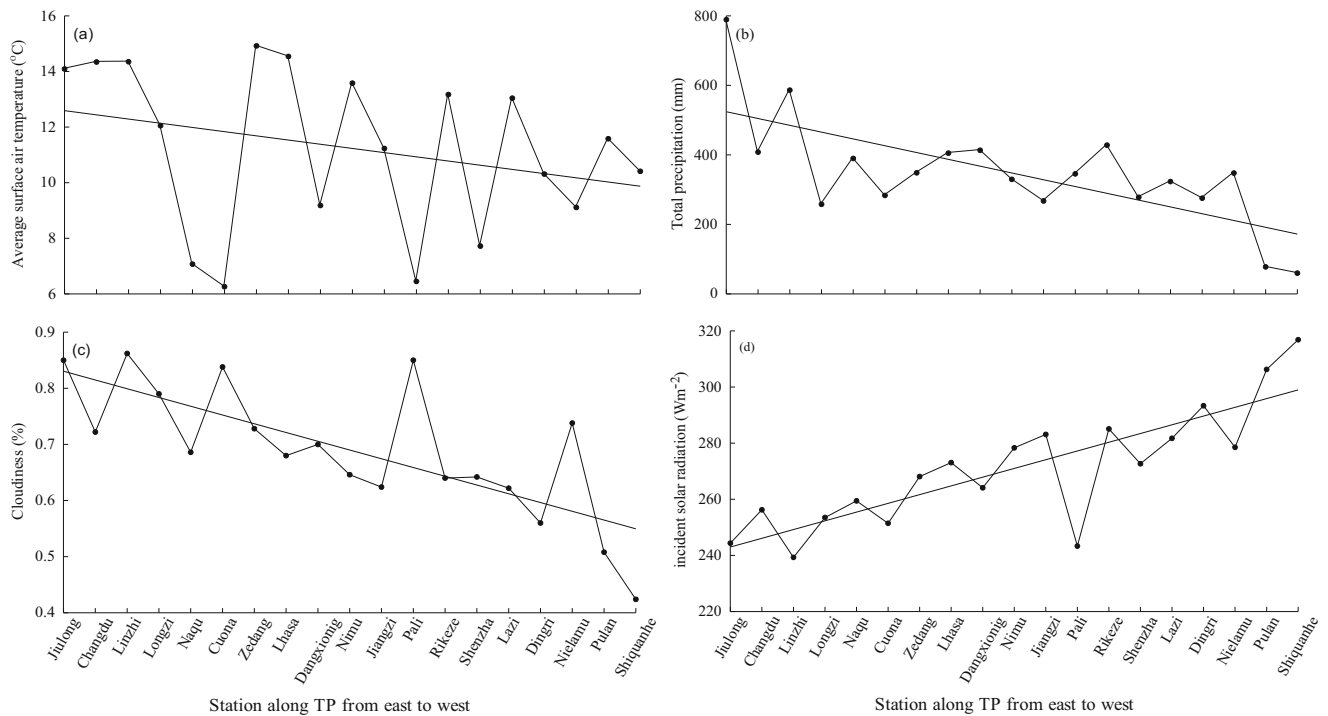


Fig. 2 Climatic background across the TP during the main growing season (May–September): **a** mean temperature (°C), **b** total precipitation (mm), **c** mean cloudiness (%), and **d** mean incident solar radiation (W m⁻²) (dashed line is the tendency estimated by linear regression)

3 Data, Model Description, and Experimental Design

3.1 Data

The atmospheric forcings required for the numerical simulation include air temperature, precipitation, wind speed, relative humidity, and downward shortwave radiation. Here, four-times-daily meteorological data from the 19 stations across the TP for the period 1981–2000, including air temperature, precipitation, relative humidity, cloudiness, and wind speed, were used as model input. Downward shortwave radiation was modified by cloudiness on the chronometer radiation because of the absence of direct observations. It was calculated as follows:

$$S_0 = 0.9S(1 - 0.55c_n) \tag{1}$$

where S_0 is incident solar radiation at the canopy top, S is incident solar radiation at the atmosphere top, and c_n is the fraction of cloudiness. Soil texture and vegetation type data were obtained using the China soil texture and vegetation type datasets (Zhang et al. 2004) with $0.1^\circ \times 0.1^\circ$ spatial resolution.

Automatic weather station data, including sensible and latent heat, land surface temperature, net radiation, and other elements, observed during 1997 and 1998 at Shiquanhe in the west of the TP as part of the China–Japan cooperative research on Asian monsoon mechanism (Li et al. 1996), were

used to evaluate the simulation skill of the atmosphere–vegetation interaction model (AVIM).

3.2 Model Description

The AVIM used in this study was a two-way interaction model comprising two modules: a physical processes module and a vegetation ecophysiological processes module. This model is constructed based on the following mechanism. The physical processes involve the water, CO₂, and energy (radiation, sensible, and latent heat) exchanges between the atmosphere, vegetation, and soil. The thermal and moisture conditions of the atmosphere can affect the growth processes of plants via physiological processes such as photosynthesis and respiration. In turn, changes of the dynamical and physical parameters of the plants can influence the water, CO₂, and energy exchanges between the atmosphere, vegetation, and soil. The major characteristic of the AVIM is that vegetation parameters such as leaf area index (LAI) and net primary production (NPP) are not prescribed but are computed by a dynamic vegetation module. The structure of the AVIM is shown in Fig. 3 (Ji 1995). The left part of the figure shows the physical processes that constitute the land surface processes module and the right part displays the plant physiological processes. This model has been used widely to simulate the physical and physiological processes for various vegetation types, e.g., temperate mixed forest, crops, and grassland (Ji 1995; Ji and

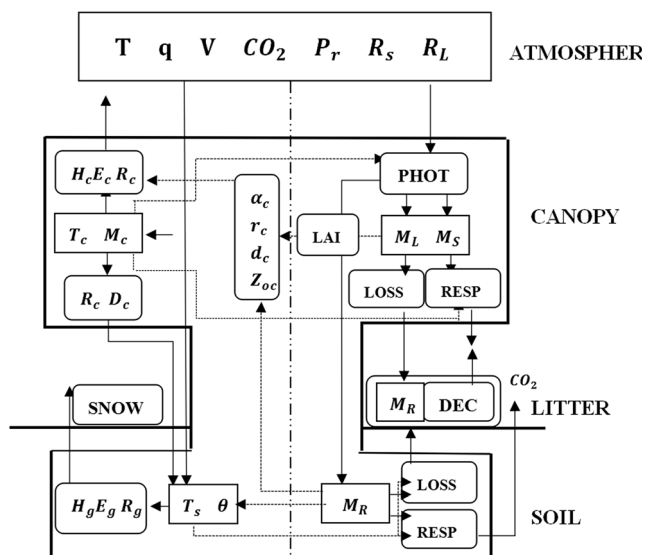


Fig. 3 Schematic of the structure of the AVIM (redrawn from Ji (1995))

Li 1999; Lu and Ji 2006), from regional to global scales. It has also been coupled with numerous climate models (Dan et al. 2002; Gao et al. 2008; Zhi et al. 2009; Wu and Coauthors 2014). A detailed description of the model can be found elsewhere (Ji 1995; Lu and Ji 2006; Huang et al. 2007a, b).

3.3 Experimental Design

The offline numerical experiments performed in the present study comprised a control simulation and two sensitivity simulations for all 19 meteorological stations that commenced on January 1, 1981 and ended on December 31, 2000. A 1-h step was set as the temporal resolution of the model output. For

model initialization, the model was cyclically spun up for 10 years with the forcing dataset of 1981. The experiments (Table 1) were performed as follows. In the control experiment (EXP1), the China vegetation type dataset (Zhang et al. 2004) was used, which represents the present-day vegetation cover over the TP. The first sensitivity simulation (EXP2) consisted of a deforestation scenario, in which we substituted all forests, high-cold steppe, and grasslands with desert steppe under the ‘worst’ scenario because of increasing desertification on the TP during recent decades (Xue et al. 2009). The second sensitivity simulation (EXP3) was a warming scenario that considered a possible change in vegetation coverage in response to climate warming on the TP during recent decades (see Section 4c for explanation of changes in vegetation coverage under the warming scenario).

4 Results

4.1 Validation of the Model

To evaluate the simulation skill of the AVIM, we first compared the simulation with automatic weather station data measured at Gaize in the west of the TP from October 1, 1997 to September 31, 1998. The agreement between the simulations and measurements is shown in Fig. 4. Simulated land surface temperature (Fig. 4a) corresponded well with the measured values. Reasonable agreement was also found for net radiation and sensible heat flux (Fig. 4b, c). Some discrepancy was found in terms of latent heat flux (Fig. 4d). Although the onset of latent heat release that accompanies the major wet season rain systems of the TP in early July was well represented by the

Table 1 Summary of the numerical experiments

Station	EXP1		EXP2		EXP3	
	Vegetation type	Vegetation coverage	Vegetation type	Vegetation coverage	Vegetation type	Vegetation coverage
Jiulong	Grasslands	0.8	Desert steppe	0.1	Same as EXP1	0.9
Changdu	High-cold steppe	0.8				0.9
Linzhi	Evergreen needle-leaf forest	0.9				0.8
Longzi	Grasslands	0.2				0.3
Naqu	High-cold steppe	0.4				0.5
Cuona	High-cold steppe	0.2				0.3
Zedang	Grasslands	0.2				0.1
Lhasa	High-cold steppe	0.8				0.6
Dangxiong	High-cold steppe	0.2				0.3
Nimu	Grasslands	0.4				0.3
Jiangzi	High-cold steppe	0.2				0.3
Pali	High-cold steppe	0.2				0.4
Rikeze	Grasslands	0.4				0.3
Shenzha	High-cold steppe	0.4				0.5
Lazi	High-cold steppe	0.2				0.1
Dingri	High-cold steppe	0.2				0.3
Nielamu	Open shrublands	0.3				0.4
Pulan	Desert steppe	0.2				0.4
Shiquanhe	Desert steppe	0.1				0.2

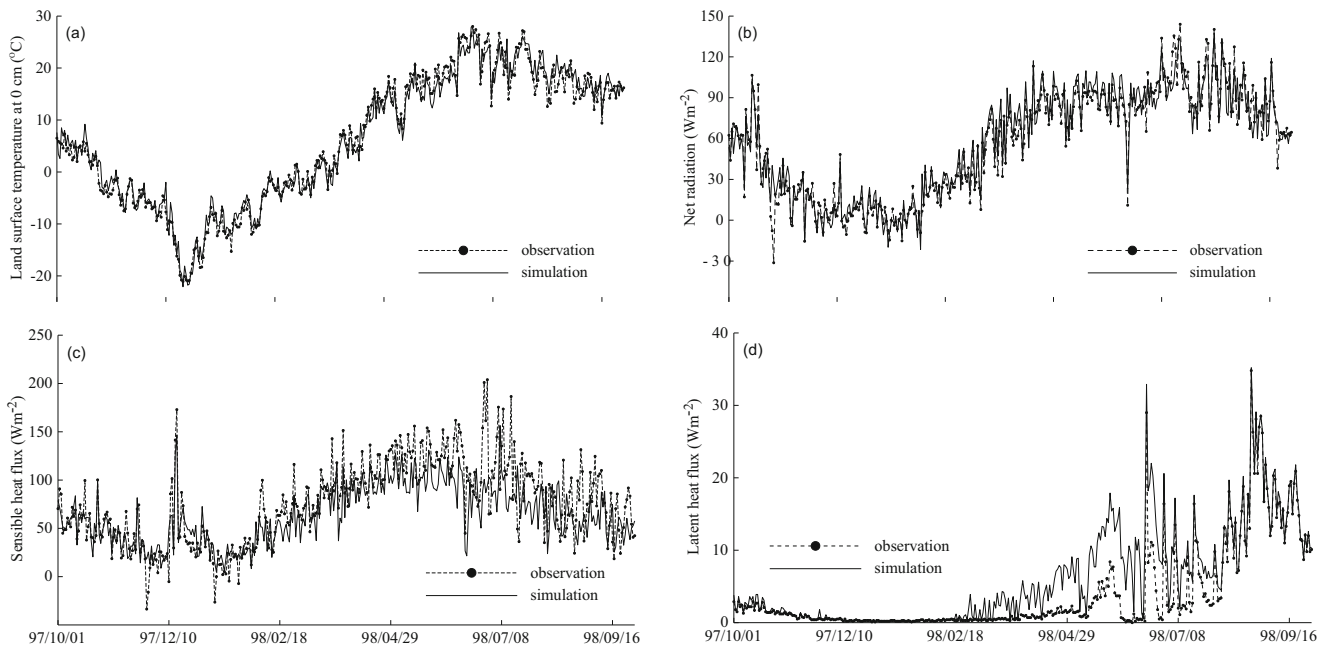


Fig. 4 Comparison of observed and simulated (a) land surface temperature (°C), (b) net radiation ($W m^{-2}$), and (c) sensible and (d) latent heat ($W m^{-2}$) at Gaize

model, its magnitude was overestimated during late winter and spring. Therefore, starting in late February 1998, the simulated latent heat flux was probably larger than measured until around mid-June. After early July, the model agreed again with the measured latent heat flux. This discrepancy appears a result of the overestimation of soil moisture (not shown) during the cold season, which was attributed partly to the proportionately large frozen soil water storage over the TP in cold seasons, because

the sensor only detects liquid water; thus, it underestimates the total water content in cold seasons. In general, the simulated results agreed well with the observations, which demonstrated the reasonable performance of the AVIM in capturing the characteristics of land–atmosphere interactions over the TP.

The climatological means of the model outputs based on a 20-year simulation are shown in Fig. 5. The NPP means the organic matter was accumulated per unit area and per unit time

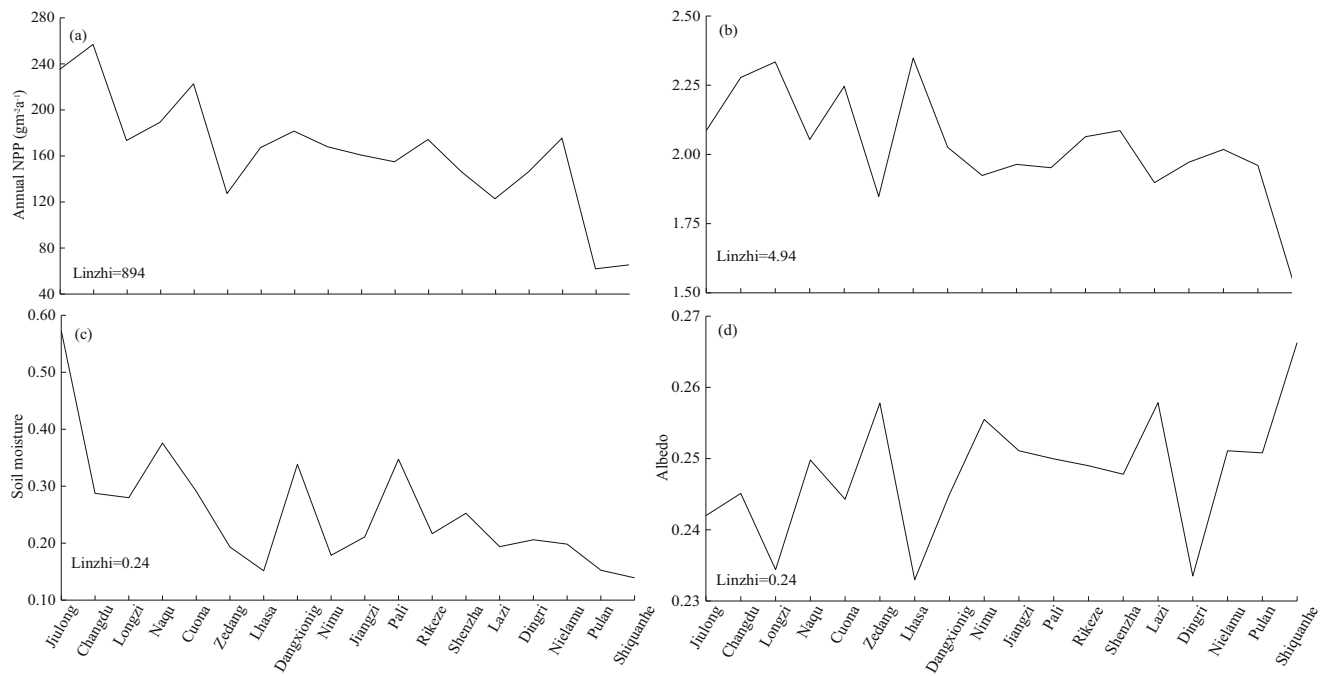
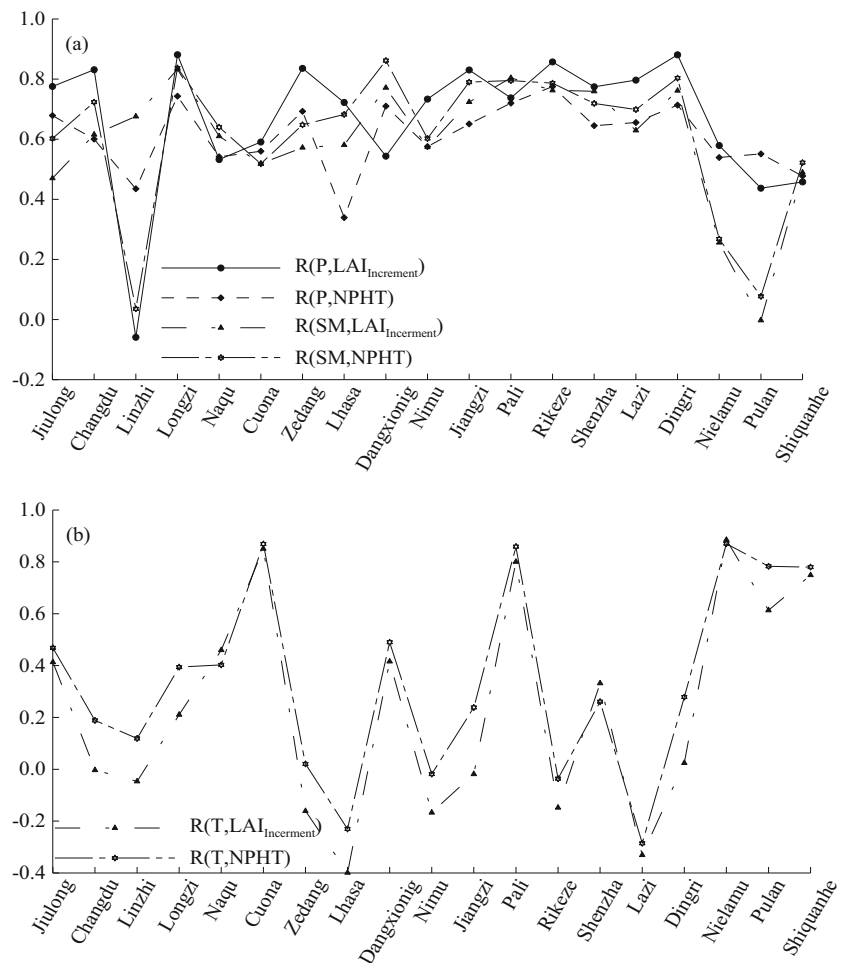


Fig. 5 Simulated distributions across the TP averaged over 1981–2000: **a** annual NPP ($g m^{-2} a^{-1}$), **b** mean LAI, **c** soil moisture of the first layer during May–September, and **d** annual mean albedo

Fig. 6 Correlations (a) between precipitation and monthly LAI increment, and soil moisture and net photosynthesis rate; and (b) between monthly surface air temperature and monthly LAI increments, and monthly surface air temperature and net photosynthesis rate across the TP



by green plants, which is an index that directly reflects the production capacity of plant communities under natural conditions. The simulated distribution of annual NPP across the

TP is shown in Fig. 5a. It can be seen that there is a strong east–west gradient of annual NPP across the TP, which ranges from about 60 to 900 g DM m⁻² a⁻¹. For example, Linzhi in the east of the TP, which is mainly covered by evergreen needleleaf forest, had the highest annual NPP of up to 894 g DM m⁻² a⁻¹. Other stations in the east of the TP, such as Jiulong and Changdu, could also exceed 240 g DM m⁻² a⁻¹. The vegetation over central areas of the TP is relatively poor in native evergreen needleleaf species compared with eastern areas. The simulated annual NPP values for the central TP were mainly 100–200 g DM m⁻² a⁻¹, while western parts of the TP had the smallest NPP values of 60–100 g DM m⁻² a⁻¹. This pattern is generally consistent with the results of Gao et al. (2013), which revealed an increase in annual NPP from western to eastern parts of the TP. The gradient of mean LAI (Fig. 5b) during the growing season was also largely consistent with that of annual NPP. The simulated mean soil moisture of the first layer during May–September and the annual mean albedo are shown in Fig. 5c, d, respectively. The soil moisture and albedo showed contrasting gradients, i.e., soil moisture decreased from east to west, whereas albedo increased from east to west.

Table 2 Regression of gross photosynthesis rate, net photosynthesis rate, and respiration rate on monthly temperature during the growing season (unit: DM m⁻² d⁻¹ K⁻¹)

Station	PHT	PHN	RESP
Jiulong	5.45	4.87	1.76
Changdu	0.80	1.82	1.31
Linzhi	11.07	5.87	7.05
Longzi	3.78	3.73	0.94
Cuona	1.98	1.60	0.85
Naqu	8.82	9.39	1.78
Zedang	-0.84	-1.32	0.45
Lhasa	-1.13	-2.98	1.32
Dangxiong	3.97	3.65	1.22
Nimu	-0.08	-1.17	0.92
Jiangzi	3.75	3.21	1.22
Pali	9.69	10.14	1.99
Rikaze	0.28	-1.01	1.14
Shenzha	2.12	1.62	0.99
Lazi	-4.05	-2.68	0.65
Dingri	2.86	3.16	0.38
Nielamu	6.31	6.25	1.63
Pulan	4.07	3.76	0.27
Shiquanhe	1.80	1.78	0.41

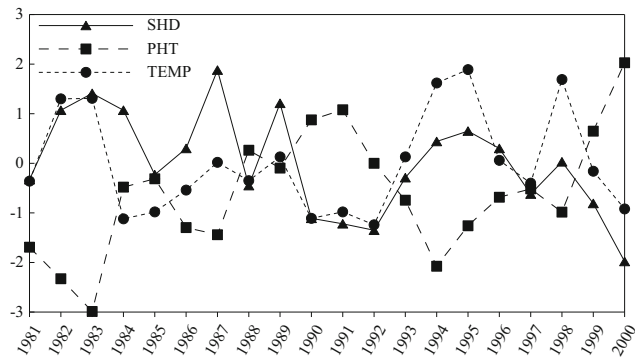


Fig. 7 May–September-averaged normalized anomalies of specific humidity deficit, air temperature, and net photosynthetic rate at Lazi

4.2 Influence of Climate Change on Vegetation

Changes to vegetation, biological or otherwise, can probably be attributed to natural causes and climate change can exert profound influence on such changes. Therefore, it is necessary to study the relationship between climate factors and vegetation growth to help us understand global change. Comparison of Fig. 5 with Fig. 2a, b shows that precipitation, temperature, and NPP have east–west gradients. This prompts us to question whether precipitation or temperature is the main climatic factor controlling vegetation growth. It is well known that higher temperature and humidity provide better conditions for vegetation growth in Alpine regions. For almost stations across the TP, the correlation coefficients between the monthly

precipitation and LAI increment during the growing season were positive and significant. The same positive correlation can also be seen in the relationship between soil moisture and net photosynthesis rate, as shown in Fig. 6a. However, it is clear that the correlation coefficients between the monthly temperature and monthly LAI increment and net photosynthesis rate of some stations, such as Changdu, Linzhi, Lhasa, Zedang, Jiangzi, Nimu, and Lazi, were weak or even negative (Fig. 6b). This suggests that climate warming might inhibit vegetation growth to some extent. However, it is unclear why negative correlation was observed between temperature and vegetation physiological processes over some areas of the TP. We next consider the effect of different climate factors on vegetation.

According to Lu and Ji (2006), the net photosynthesis rate is influenced by temperature via the following mechanisms. 1) The maximum carboxylation rate is determined directly by foliage temperature (i.e., the higher the temperature, the higher the maximum carboxylation rate). This indicates an increase in temperature results in an enhanced maximum carboxylation rate and an increase in the net photosynthesis rate. 2) The temperature can affect the respiration rate of the vegetation. Increased temperature can lead to an increased respiration rate, which could then inhibit vegetation growth. 3) The temperature can influence the leaf–air specific humidity deficit (similar to the vapor pressure deficit). The humidity difference depends on the foliage temperature and air humidity. A decrease in humidity difference will reduce the degree of stomatal closure, increasing the CO₂ concentration, which is

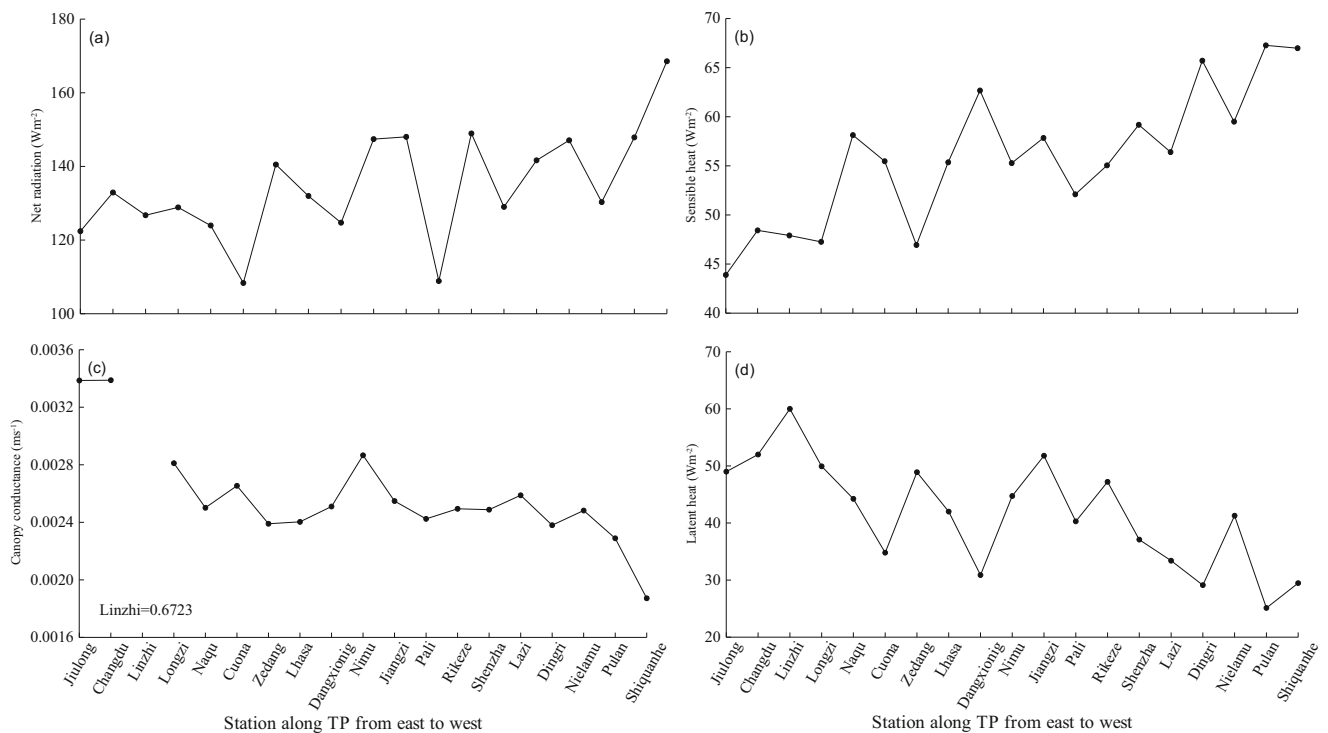
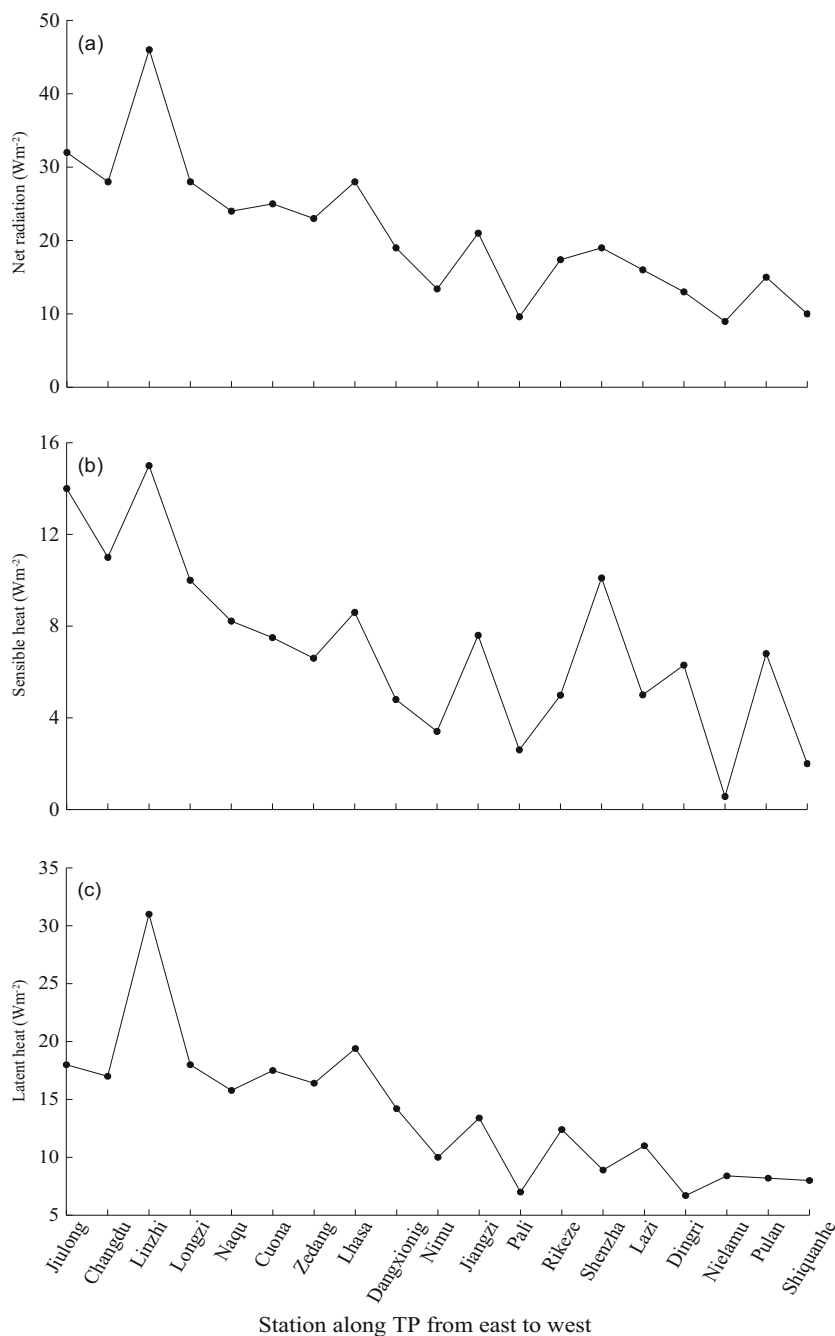


Fig. 8 Same as Fig. 5 but for the mean (a) net radiation ($W m^{-2}$), (b) sensible heat ($W m^{-2}$), (c) canopy conductance ($m s^{-1}$), and (d) latent heat ($W m^{-2}$) during May–September

Fig. 9 Mean of difference of (a) net radiation (W m^{-2}), (b) sensible heat flux (W m^{-2}), and (c) latent heat flux (W m^{-2}) between EXP2 and EXP1 during May–September



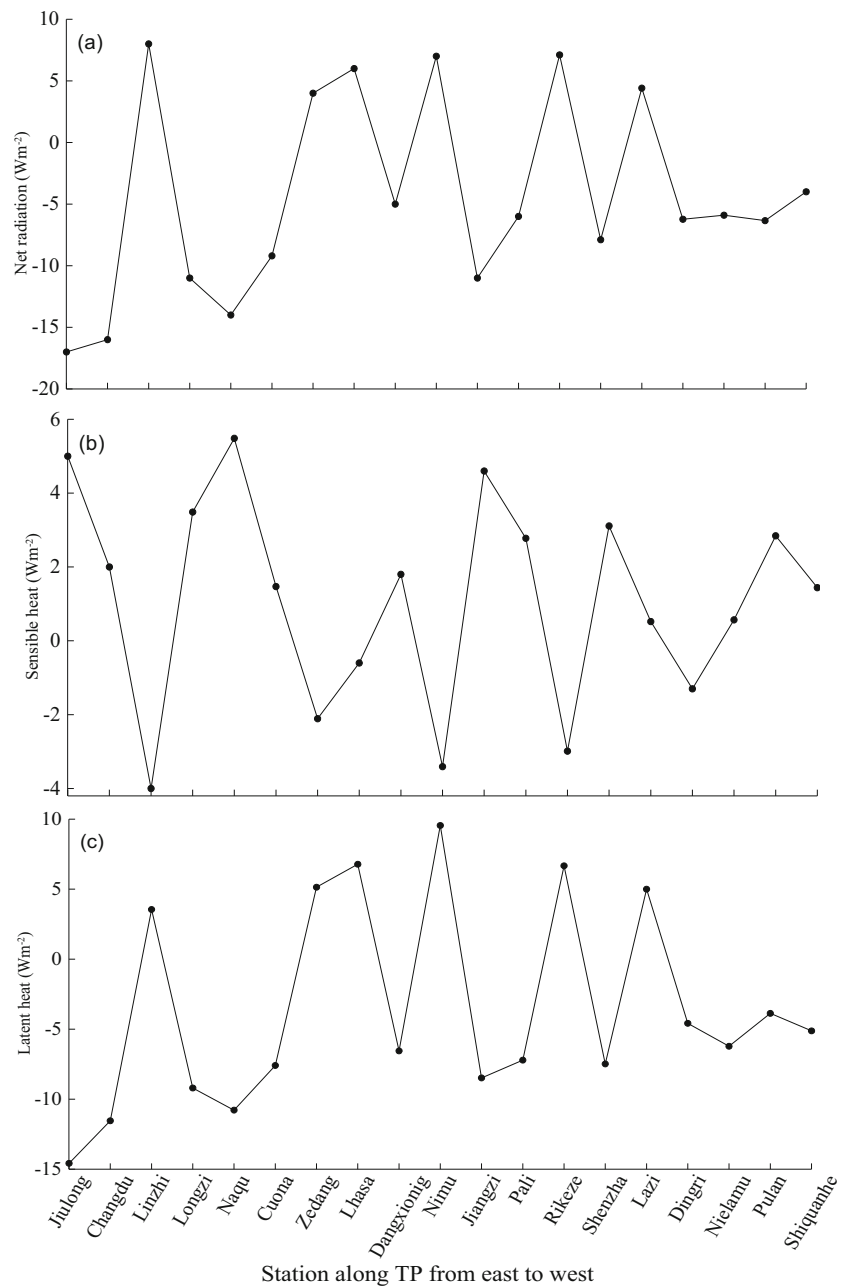
beneficial to photosynthesis and ultimately affects evaporation. Therefore, a higher temperature can increase the specific humidity deficit and further reduce the intercellular CO_2 concentration C_i . However, a lower C_i means a lower Rubisco-limited carboxylation rate and a carboxylation rate limited by RuBP regeneration; thus, the photosynthesis rate or vegetation growth will be lower under higher temperatures.

If mechanism 1 dominates, positive correlation between temperature and net photosynthesis for all stations could be expected. However, some stations with negative correlation are shown in Fig. 6, which cannot be explained under

mechanism 1. If, however, mechanisms 2 and 3 dominate, this negative correlation could be explained. To distinguish the main mechanism for each station with negative correlation, we calculated the regression of the gross photosynthesis rate, net photosynthesis rate, and respiration rate on temperature (Table 2) to quantify the relative importance of the latter two mechanisms.

Table 2 shows that for most stations across the TP, an increase in temperature could significantly increase the physiological activity of vegetation, including the gross photosynthesis rate, net photosynthesis rate, and respiration rate.

Fig. 10 Same as Fig. 9 but for mean of the difference between EXP3 and EXP1



Furthermore, the increments of total photosynthetic rate and net photosynthetic rate were higher than that of respiration rate, indicating that mechanism 1 is the major pathway via which temperature affects the vegetation at these stations. For Linzhi, in the east of the TP, a 1 °C warming could increase the net photosynthesis rate by 5.87 g DM m⁻² d⁻¹ but it could also increase the respiration rate by 7.05 g DM m⁻² d⁻¹. This suggests that climate warming not only increases vegetation photosynthesis but also, even more markedly, increases respiration, especially in areas where water and heat are relatively plentiful. Thus, we can conclude that mechanism 2 accounts for the weak positive and negative correlation between temperature and vegetation growth at Linzhi. At other

stations, such as Lhasa, Zedang, Nimu, Rikaze, and Lazi, where the elevation is relatively lower (mainly <4000 m) and the climate is relatively warmer but not wetter, 1 °C warming increased the respiration rate from 0.45 to 1.32 g DM m⁻² d⁻¹. This also reduced the net photosynthesis rate by 1.01 to 2.98 g DM m⁻² d⁻¹. In these cases, temperature affected photosynthesis via an indirect relationship: the temperature first influenced the moisture condition of the vegetation via change in the leaf–air specific humidity deficit, which then influenced photosynthesis. Here, Lazi was taken as an example to explore this mechanism and to illustrate how temperature influences vegetation growth. Figure 7 shows the May–September-averaged normalized anomalies of specific

humidity deficit, air temperature, and net photosynthetic rate at Lazi. The anomalies of specific humidity deficit and temperature during the growing season showed significant positive correlation, while significant negative correlation was found between specific humidity deficit and net photosynthetic rate. This suggests that mechanism 3, i.e., change in the photosynthetic process caused by temperature, rather than change in the respiration process, is the most important cause of the negative correlation between temperature and vegetation growth.

4.3 Influence of Vegetation Change on Land Surface Physical Processes

It is well known that the distribution of surface physical fluxes is determined primarily by climate state. The net radiation fluxes and sensible heat fluxes across the TP show a gradient with highest values in the west and lowest values in the east (Fig. 8a, b). This pattern is the opposite to the distribution of temperature, precipitation, and cloudiness and similar to that of incident solar radiation. In addition, the distribution of physical fluxes depends not only on the climate state but also on the vegetation species, coverage, and associated canopy structures, leaf area, and other related factors. In these cases, canopy conductance (i.e., the reciprocal of canopy resistance) associated with vegetation physiology is an important factor controlling the partitioning of sensible and latent fluxes. If canopy conductance is large (or the corresponding resistance is small), the partitioning of net radiation relative to latent heat will be high, and vice versa. It can be seen from Fig. 8c that the distribution of canopy conductance was much greater over the eastern TP than over the west. Linzhi, in the east of the TP, had the largest canopy conductance of $6.70 \times 10^{-3} \text{ m s}^{-1}$, whereas Shiquanhe, in the west of the TP, had the smallest canopy conductance ($1.87 \times 10^{-3} \text{ m s}^{-1}$); thus, the latent heat flux decreased from east to west (Fig. 8d).

The analysis above clearly indicates that the physical fluxes across the TP could be influenced considerably by vegetation condition. This was explored further via two sensitivity experiments in which the vegetation of all 19 stations was assumed degenerated to desert steppe (EXP2), and vegetation coverage was shifted in response to climate warming (EXP3). Figure 9 shows the difference in surface heat fluxes between EXP1 and EXP2. A clear difference in net radiation can be seen for all stations because of the presence of vegetation. The maximum difference was 47 W m^{-2} at Linzhi, which almost reached 38% of net radiation (Fig. 9a). Furthermore, both the sensible and the latent heat fluxes in EXP1 were larger than in EXP2 because more radiation is absorbed when vegetation is present. This effect was particularly clear at Linzhi in the east of the TP, where the main vegetation type is evergreen needleleaf forest (Fig. 9b, c). Thus, it implies that desertification could

contribute to climate change by playing an important role in weakening surface heat sources.

It is important to stress that EXP2 is the ‘worst’ scenario and that it is very unlikely to occur in reality. The analysis of the influence of climate change on vegetation in Section 4b shows that the response of vegetation to climate change differs depending on geographical location and the magnitude of the climate change. Warming has caused an increase in photosynthesis at most stations across the TP with increased plant growth; however, photosynthesis has been restrained in some regions, such as Linzhi, Lazi, and Lasa, slowing plant growth. Thus, we modified the vegetation coverage for each station other than the drastic changes in land cover, according to its response to climate warming, as discussed in Section 4b. The regionality of the response to vegetation coverage was particularly varied for surface heat fluxes (Fig. 10). In most areas, an increase in vegetation fraction would increase the LAI but decrease the surface albedo, resulting in greater absorption of radiation by the land surface, and this difference exhibited a clear east–west gradient (Fig. 10a). It would also marginally increase the surface roughness, which would result in a small reduction of sensible heat from east to west (Fig. 10b). For latent heat, although a higher vegetation fraction has potential to decrease soil evaporation markedly via reduced soil temperature and shortwave radiation; vegetation transpiration was found much greater from east to west in EXP3 because of increased shading by vegetation, which contributed to the larger latent heat flux of EXP3 in comparison with EXP1 (Fig. 10c). This relationship was reversed in other regions where plant growth was depressed by higher temperature. Therefore, although the changes in vegetation physiological processes in response to climate warming varied depending on geographical location, climate warming during recent decades could be expected to have accelerated vegetation growth in most areas of the TP, further increasing the surface heat flux of the TP from east to west.

5 Summary and Discussion

The TP is an important region of land–atmosphere interactions. This study considered the possible responses of vegetation to climate warming over the TP and it evaluated the impact of LCC from vegetated land to bare ground (i.e., land degradation) on the land surface physical processes using the AVIM. We found the response of vegetation to long-term warming over the TP occurred via different mechanisms. In general, climatic warming will benefit vegetation growth for most high cold areas of the TP; however, it will inhibit vegetation growth by increasing respiration, especially in areas with sufficient water supply and suitable temperature. In addition, climatic warming could affect the photosynthesis rate via the moisture condition of the vegetation rather than by

modulating respiration. The effects of idealized land degradation on the TP demonstrated that vegetation could control the land surface–atmosphere energy balance effectively, and that LCC from vegetated land to bare ground would decrease the net radiation absorbed by the surface, resulting in weaker surface thermal effects, and leading to lower sensible and latent heat fluxes. Furthermore, although the changes in vegetation physiological processes in response to climate warming varied depending on geographical location, the climate warming during recent decades could be expected to have accelerated vegetation growth in most areas of the TP, further increasing the surface heat flux of TP.

Some important problems remain unresolved. Although not a focus of this study, to improve the understanding of the vegetation–climate feedbacks on the TP, future work should investigate the influence of vegetation phenology on the TP. For example, the extent to which climate warming might affect growing day characteristics remains unclear. Furthermore, our simulations were based on meteorological station observations rather than high-resolution gridded datasets. Therefore, for minimization of the simulation uncertainties in further work, high-resolution data should be used as input.

Acknowledgements This work was funded by the National Science Foundation of China (41775072, 91537214, 41405069, 41605063 and 41705065), the Key Foundation of the Education Department of Sichuan Province (16ZA0203), and the Scientific Research Foundation of Chengdu University of Information Technology (J201516 and J201518). We acknowledge the critical comments from anonymous reviewers and editor.

References

- Cramer, W., Coauthors: Global response of terrestrial ecosystem structure and function to CO₂ and climate change: results from six dynamic global vegetation models. *Glob. Chang. Biol.* **7**, 357–373 (2001). <https://doi.org/10.1046/j.1365-2486.2001.00383.x>
- Crucifix, M., Betts, R.A., Cox, P.M.: Vegetation and climate variability: a GCM modelling study. *Clim. Dyn.* **24**, 457–467 (2005). <https://doi.org/10.1007/s00382-004-0504-z>
- Dan, L., Ji, J., Li, Y.: Climate simulate based on a different-grid nested and coupled model. *Adv. Atmos. Sci.* **19**, 487–499 (2002). <https://doi.org/10.1007/s00376-002-0081-1>
- Duan, A., Wu, G.: Weakening trend in the atmospheric heat source over the Tibetan plateau during recent decades. Part I: observations. *J. Clim.* **21**, 3149–3164 (2008). <https://doi.org/10.1175/2007JCLI1912.1>
- Flohn, H.: Large-scale aspects of the “summer monsoon” in south and East Asia. *J. Meteorol. Soc. Jpn.* **75**, 180–186 (1957). https://doi.org/10.2151/jmsj1923.35A.0_180
- Gao, R., Dong, W., Wei, Z.: Simulation and analysis of China climate using two-way interactive atmosphere-vegetation model (RIEMS-AVIM). *Adv. Atmos. Sci.* **25**, 1085–1097 (2008). <https://doi.org/10.1007/s00376-008-1085-2>
- Gao, Y., Zhou, X., Wang, Q., Wang, C., Zhan, Z., Chen, L., Yan, J., Qu, R.: Vegetation net primary productivity and its response to climate change during 2001–2008 in the tibetan plateau. *Sci. Total. Environ.* **444**, 356–362 (2013). <https://doi.org/10.1016/j.scitotenv.2012.12.014>
- Goetz, S.J., Prince, S.D., Small, J., Gleason, A.C.R.: Interannual variability of global terrestrial primary production: results of a model driven with satellite observations. *J. Geophys. Res. Atmos.* **105**, 20077–20091 (2000)
- Guo, D., Wang, H.: The significant climate warming in the northern Tibetan plateau and its possible causes. *Int. J. Climatol.* **32**, 1775–1781 (2012). <https://doi.org/10.1002/joc.2388>
- Hua, W., Fan, G., Zhou, D., Ni, C., Li, X., Wang, Y., Liu, Y., Huang, X.: Preliminary analysis on the relationships between tibetan plateau ndvi change and its surface heat source and precipitation of China. *Sci. China Ser. D.* **51**, 677–685 (2008). <https://doi.org/10.1007/s11430-008-0063-y>
- Hua, W., Fan, G., Yang, K.: Uncertainty in hottest years ranking: analysis of Tibetan plateau surface air temperature. *Atmos. Oceanic. Sci. Lett.* **10**, 337–341 (2017)
- Huang, M., Ji, J., Li, K., Liu, Y., Yang, F., Tao, B.: The ecosystem carbon accumulation after conversion of grasslands to pine plantations in subtropical red soil of South China. *Tellus B.* **59**, 439–448 (2007a). <https://doi.org/10.1111/j.1600-0889.2007.00280.x>
- Huang, M., Ji, J., Li, K., Liu, Y., Yang, F., Tao, B.: The ecosystem carbon accumulation after conversion of grasslands to pine plantations in subtropical red soil of South China. *Tellus B.* **59**, 439–448 (2007b). <https://doi.org/10.1111/j.1600-0889.2007.00280.x>
- Ji, J.: A climate-vegetation interaction model: simulating physical and biological processes at the surface. *J. Biogeogr.* **22**, 445–451 (1995). <https://doi.org/10.2307/2845941>
- Ji, J., Li, Y.: A simulation study of coupled feedback mechanism between physical and biogeochemical processes at surface. *Chinese J. Atmos. Sci.* **23**, 439–448 (1999) (in Chinese)
- Jones, P.D., Lister, D.H., Osborn, T.J., Harpham, C., Salmon, M., Morice, C.P.: Hemispheric and large-scale land-surface air temperature variations: an extensive revision and an update to 2010. *J. Geophys. Res.* **117**, D05127 (2012). <https://doi.org/10.1029/2011JD017139>
- Lenihan, J.M., Bachelet, D., Neilson, R.P., Drapek, R.: Response of vegetation distribution, ecosystem productivity, and fire to climate change scenarios for California. *Clim. Chang.* **87**, 215–230 (2008). <https://doi.org/10.1007/s10584-007-9362-0>
- Li, C., Yanai, M.: The onset and interannual variability of the Asian summer monsoon in relation to land-sea thermal contrast. *J. Clim.* **9**, 358–375 (1996). [https://doi.org/10.1175/1520-0442\(1996\)009<0358:TOAIVO>2.0.CO;2](https://doi.org/10.1175/1520-0442(1996)009<0358:TOAIVO>2.0.CO;2)
- Li, G., Duan, T., Wan, J., Gong, Y., Shigenori, H., Chen, L., Li, W.: Determination of the drag coefficient over the Tibetan plateau. *Adv. Atmos. Sci.* **13**, 511–518 (1996). <https://doi.org/10.1007/BF03422041>
- Li, Q., Xue, Y.: Simulated impacts of land cover change on summer climate in the Tibetan plateau. *Environ. Res. Lett.* **5**, 015102 (2010). <https://doi.org/10.1088/1748-9326/5/1/015102>
- Lu, J., Ji, J.: A simulation and mechanism analysis of long-term variations at land surface over arid/semi-arid area in North China. *J. Geophys. Res. Atmos.* **111**, D09306 (2006). <https://doi.org/10.1029/2005JD006252>
- Notaro, M., Liu, Z.: Statistical and dynamical assessment of vegetation feedbacks on climate over the boreal forest. *Clim. Dyn.* **31**, 691–712 (2008). <https://doi.org/10.1007/s00382-008-0368-8>
- Pearson, R.G., Phillips, S.J., Loranty, M.M., Beck, P.S.A., Damoulas, T., Knight, S.J., Goetz, S.J.: Shifts in Arctic vegetation and associated feedbacks under climate change. *Nat. Clim. Chang.* **3**, 673–677 (2013). <https://doi.org/10.1038/nclimate1858>
- Theurillat, J.P., Guisan, A.: Potential Impact of Climate Change on Vegetation in the European Alps: A Review. *Clim. Chang.* **50**, 77–109 (2001). <https://doi.org/10.1023/A:1010632015572>
- Wang, Z., Duan, A., Wu, G.: Time-lagged impact of spring sensible heat over the Tibetan plateau on the summer rainfall anomaly in East China: case studies using the WRF model. *Clim. Dyn.* **42**, 2885–2898 (2014). <https://doi.org/10.1007/s00382-013-1800-2>

- Wang, Z., Duan, A., Wu, G., Yang, S.: Mechanism for occurrence of precipitation over the southern slope of the Tibetan plateau without local surface heating. *Int. J. Climatol.* **36**, 4164–4171 (2016). <https://doi.org/10.1002/joc.4609>
- Wang, Z., Duan, A., Yang, S.: Potential regulation on the climatic effect of Tibetan plateau heating by tropical air-sea coupling in regional models. *Clim. Dyn.* (2018). <https://doi.org/10.1007/s00382-018-4218-z>
- Wu, T., Coauthors: An overview of BCC climate system model development and application for climate change studies. *J. meteor. Res.* **28**, 34–56 (2014). <https://doi.org/10.1007/s13351-014-3041-7>
- Xue, X., Jian, G., Han, B., Sun, Q., Liu, L.: The effect of climate warming and permafrost thaw on desertification in the Qinghai-Tibetan plateau. *Geomorphology*. **108**, 182–190 (2009). <https://doi.org/10.1016/j.geomorph.2009.01.004>
- Yanai, M., Li, C., Song, Z.: Seasonal heating of the Tibetan plateau and its effects on the evolution of the Asian summer monsoon. *J. meteorol. Soc. Jpn.* **70**, 419–434 (1992). https://doi.org/10.2151/jmsj1965.70.1B_319
- Yeh, T., Luo, L., Zhu, B.: The heat balance of the flow structure and the troposphere and near the Tibetan plateau. *J. meteorol.* **28**, 108–121 (1957) (in Chinese)
- Zhang, J., Wu, L., Huang, G., Zhu, W., Zhang, Y.: The role of May vegetation greenness on the southeastern Tibetan plateau for East Asian summer monsoon prediction. *J. Geophys. Res. Atmos.* **116**, D05106 (2011). <https://doi.org/10.1029/2010JD015095>
- Zhang, S., Peng, G., Huang, M.: The feature extraction and data fusion of regional soil textures based on GIS techniques. *Clim. Environ. Res.* **6**, 65–79 (2004) (in Chinese)
- Zhao, D., Wu, S.: Responses of vegetation distribution to climate change in China. *Theor. Appl. Climatol.* **117**, 15–28 (2014). <https://doi.org/10.1007/s00704-013-0971-4>
- Zhao, P., Chen, L.: Climate features of atmospheric heat source/sink over the Qinghai-Xizang plateau in 35 years and its relation to rainfall in China. *Sci. China. Ser. D.* **44**, 858–864 (2001). <https://doi.org/10.1007/BF02907098>
- Zhi, H., Wang, P., Dan, L., Yu, Y., Xu, Y., Zheng, W.: Climate-vegetation interannual variability in a coupled atmosphere-ocean-land model. *Adv. Atmos. Sci.* **26**, 599–612 (2009). <https://doi.org/10.1007/s00376-009-0599-6>
- Zhong, L., Ma, Y., Salama, M., Su, Z.: Assessment of vegetation dynamics and their response to variations in precipitation and temperature in the Tibetan plateau. *Clim. Chang.* **103**, 519–535 (2010). <https://doi.org/10.1007/s10584-009-9787-8>
- Zhou, B., Wen, Q., Xu, Y., Song, L., Zhang, X.: Projected changes in temperature and precipitation extremes in China by the CMIP5 multi-model ensembles. *J. Clim.* **27**, 6591–6611 (2014). <https://doi.org/10.1175/JCLI-D-13-00761.1>
- Zuo, Z., Zhang, R., Zhao, P.: The relation of vegetation over the Tibetan plateau to rainfall in China during the boreal summer. *Clim. Dyn.* **36**, 1207–1219 (2011). <https://doi.org/10.1007/s00382-010-0863-6>